Atmos. Chem. Phys. Discuss., 15, 27627–27673, 2015
www.atmos-chem-phys-discuss.net/15/27627/2015/
doi:10.5194/acpd-15-27627-2015

Atmospheric Chemistry and Physics
Discussions
Open Access

Characterization of total ecosystem scale biogenic VOC exchange at a Mediterranean oak-hornbeam forest

S. Schallhart[1], **P. Rantala**[1], **E. Nemitz**[2], **D. Mogensen**[1], **R. Tillmann**[3], **T. F. Mentel**[3], **J. Rinne**[1,4,5], and **T. M. Ruuskanen**[1]

[1]Department of Physics, University of Helsinki, Helsinki, Finland
[2]Centre for Ecology and Hydrology (CEH), Penicuik, UK
[3]Forschungszentrum Juelich GmbH, Juelich, Germany
[4]Department of Geosciences and Geography, University of Helsinki, Helsinki, Finland
[5]Finnish Meteorological Institute, Helsinki, Finland

Received: 21 August 2015 – Accepted: 17 September 2015 – Published: 14 October 2015

Correspondence to: S. Schallhart (simon.schallhart@helsinki.fi)

Published by Copernicus Publications on behalf of the European Geosciences Union.

Abstract

Recently, the number and amount of biogenically emitted volatile organic compounds (VOCs) has been discussed vigorously. Depending on the ecosystem the published number varies between a dozen and several hundred compounds. We present ecosystem exchange fluxes from a mixed oak-hornbeam forest in the Po Valley, Italy. The fluxes were measured by a proton transfer reaction-time-of-flight (PTR-ToF) mass spectrometer and calculated by the eddy covariance (EC) method. Detectable fluxes were observed for twelve compounds, dominated by isoprene, which comprised over 65 % of the total flux emission. The daily average of the total VOC emission was 9.5 $\mathrm{nmol\,m^{-2}\,s^{-1}}$. Methanol had the highest concentration and accounted for the largest deposition. Methanol seemed to be deposited to dew, as the deposition happened in the early morning, right after the calculated surface temperature came closest to the calculated dew point temperature.

We estimated that up to 27 % of the upward flux of methyl vinyl ketone (MVK) and methacrolein (MACR) originated from atmospheric oxidation of isoprene. A comparison between two flux detection methods (classical/visual and automated) was made. Their respective advantages and disadvantages were discussed and the differences in their results shown. Both provide comparable results; however we recommend the automated method with a compound filter, which combines the fast analysis and better flux detection, without the overestimation due to double counting.

1 Introduction

Volatile organic compound- fluxes between vegetation and atmosphere affect atmospheric chemistry by controlling the oxidation capacity of the atmosphere (Fehsenfeld et al., 1992; Fuentes et al., 2000). The non-methane biogenic VOC emissions are dominated by terpenoids, e.g. isoprene and monoterpenes, followed by oxygenated VOCs such as methanol and acetone (Kesselmeier et al., 1999; Guenther et al., 2012). The emitted VOCs are physically removed by dry or wet deposition or are oxidized by e.g. OH, O_3 and NO_3 (Mogensen et al., 2015). Their oxidation contributes to the tropospheric ozone formation and destruction processes (e.g. Derwent et al., 2003; Bloss et al., 2005), aerosol formation and aerosol growth and, thereby, influences air quality and climate (Kulmala et al., 1998; Tunved et al., 2006; Monks et al., 2009; Riipinen et al., 2012; Paasonen et al., 2013). To assess these effects caused by the biogenic VOCs, reliable flux budgets are necessary.

Most ecosystem scale VOC emission measurements have been conducted with disjunct eddy covariance method by mass scanning using proton-transfer-reaction quadrupole-mass-spectrometer (PTR-QMS), or relaxed eddy accumulation or surface layer gradient techniques with gas chromatography–mass spectrometry applying selected ion mode (e.g. Lamb et al., 1985; Businger and Oncley, 1990; Fuentes et al., 1996; Guenther et al., 1996; Rinne et al., 2001; Karl et al., 2002; Rinne and Ammann, 2012). These methods require pre-selection of target compounds and in case of the PTR-QMS suffer from the limitation of unit mass resolution, making it impossible to separate isobaric compounds, i.e. compounds with identical integer mass, but different chemical composition. Thus, measurements inherently focused on compounds already known to be emitted by vegetation and thereby hinder the discovery of fluxes of compounds not previously known to be emitted by vegetation. Furthermore, extreme weather conditions like hail can change the VOC flux pattern (Kaser et al., 2013), which is difficult to measure with such methods.

Lately, new insights were provided by the more universal and sensitive PTR-ToF. Park et al. (2013) analysed flux data obtained by the PTR-ToF and revealed many previously unobserved compounds to be emitted, but this approach has so far only been applied to very few vegetation types (e.g. Ruuskanen et al., 2011; Park et al., 2013; Kaser et al., 2013).

In this study we have conducted VOC flux measurements at a remnant natural oak-hornbeam dominated forest (Bosco Fontana) in northern Italy as part of an intensive field campaign organized by the European FP7 project “ÉCLAIRE” (Effects of climate change on air pollution impacts and response strategies for European ecosystems). The objectives of the ÉCLAIRE Bosco Fontana experiment were (a) to quantify the exchange of a range of pollutants with this ecosystem in one of the most polluted regions of Europe, (b) to assess the importance of in-canopy chemical interactions on the biosphere/atmosphere exchange of reactive gases and aerosols and (c) to provide a supersite in the framework of a spatial Po Valley study that combined resources from two EU projects (ÉCLAIRE, PEGASOS: Pan-European gas aerosol climate interaction study) with a national Italian initiative.

In this paper we present the results of the application of state-of-the-art PTR-ToF mass spectrometry and eddy covariance technique to derive the total biogenic VOC flux above the Bosco Fontana ecosystem. The aims of this study were: (i) the comparison of two data processing approaches to identify compounds for which fluxes were above the detection limit, contrasting the automated method used by Park et al. (2013) with the classical method using manual cross covariance peak checking (e.g. Taipale et al., 2010; Ruuskanen et al., 2011; Kaser et al., 2013), (ii) the characterization of the ecosystem scale total VOC emissions from a Mediterranean oak forest, with particular emphasis on (iii) the quantification of the contribution of non-terpenoid VOCs to the total VOC emission, (iv) the estimation of the possible contribution of secondary compounds to the observed above-canopy fluxes, and (v) the study of the dew potentially causing the methanol deposition in the mornings.

A companion paper (Acton et al., 2015) compares the PTR-ToF-MS measurements with simultaneous measurements by PTR-QMS and a bottom-up estimate of the canopy flux scaled up from leaf level emission measurements, and also derives emission factors for the use in emissions models.

2 Materials and methods

2.1 Bosco Fontana site description

The measurements were performed from 15 June to 6 July 2012 in Bosco Fontana, Lombardy, Italy. Bosco Fontana is a 233 ha forested nature reserve located in the north-east of the Po valley. The main tree species are *Quercus cerris* (turkey oak), *Quercus robur* (pedunculate oak), *Quercus rubra* (northern red oak) and *Carpinus betulus* (Hornbeam) (Dalponte et al., 2008). The typical height of the trees varied between 26 and 28 m. The surroundings of the Bosco Fontana forest area are agricultural land and some roads. The largest city nearby is Mantua, with 48 000 inhabitants, which is located 8 km to the south-east. The measurement site is 25 m a.s.l. The temperatures varied from 18 to 32 °C during the campaign and the main wind directions were east and west (Fig. 6a). The measurement tower was 42 m high and located in the south-western part of the nature reserve (45.20° N, 10.74° E; Fig. 1). The climatological mean annual temperature is 13.3 °C and the mean annual precipitation is 834 mm (Willmott and Matsuura, 2012a, b).

2.2 Meteorological and trace gas data

The measurement tower was equipped with temperature and relative humidity sensors at several heights. The turbulence data were measured with a 3-D anemometer (HS 50, Gill Instruments, UK) at 32 m above ground level (later referred as a.g.l.). An additional measurement of wind direction was provided by a 2-D ultrasonic anemometer as part of an integrated weather station (Weather Transmitter WXT610, Vaisala, Vantaa, Finland; 32 m a.g.l.), which also measured air pressure, relative humidity and temperature. The O_3 concentration was determined with a chemiluminescence analyser (Model 202, 2B Technologies) at 40 m a.g.l. and NO_2 and NO with a chemiluminescence analyser equipped with a thermal converter (Model 42C, Thermo Scientific) at a height of 32 m a.g.l.

The dew point temperature, T_d, was calculated according to Lawrence (2005):

$$T_\mathrm{d} = T\left[1 - \frac{T\ln\left(\frac{\mathrm{RH}}{100}\right)}{\frac{L_\mathrm{vap}}{R_\mathrm{w}}}\right]^{-1} \tag{1}$$

where T is the ambient temperature, RH is the relative humidity, L_vap is the enthalpy of vaporization ($2.501 \times 10^6\,\mathrm{J\,kg^{-1}}$) and R_w is the gas constant of water vapour ($461.5\,\mathrm{J\,K^{-1}\,kg^{-1}}$).

The average leaf surface temperature $T\left(z_0'\right)$ was estimated using a method described by Nemitz et al. (2009) as

$$T\left(z_0'\right) = T + \overline{\theta' w'}(R_a + R_b), \tag{2}$$

where z_0' is the notional mean height of the canopy exchange, $\overline{\theta' w'}$ and T are the measured heat flux and temperature at the measurement height of z_m, respectively. In this study, the roughness length z_0 was estimated to be ca. 1 m (e.g. Dolman, 1986). For the zero displacement height d we used the common approximation of $d = 2/3 \cdot z_\mathrm{c}$, where z_c is the canopy height (28 m).

The resistance parameters R_a and R_b were determined as (Garland, 1977; Owen and Thompson, 1963)

$$R_a = \frac{u}{u_*^2} - \frac{\Psi_\mathrm{h}\left(\frac{z_\mathrm{m}-d}{L}\right) - \Psi_\mathrm{m}\left(\frac{z_\mathrm{m}-d}{L}\right)}{ku_*} \tag{3}$$

and

$$R_b = (Bu_*)^{-1}, \tag{4}$$

where L is the Obukhov length. The sublayer-Stanton number (B) can be estimated by

$$B^{-1} = 1.45 Re_*^{0.24} Sc^{0.8}, \tag{5}$$

Title Page
Abstract | Introduction
Conclusions | References
Tables | Figures
I◀ | ▶I
◀ | ▶
Back | Close
Full Screen / Esc
Printer-friendly Version
Interactive Discussion

where roughness Reynolds number Re_* is given by

$$Re_* = \frac{z_0 u_*}{\upsilon} \tag{6}$$

and the Schmidt number Sc by

$$Sc = \frac{\upsilon}{D} \tag{7}$$

The friction velocity u_* and the horizontal wind u were taken from the measurements at z_m and k is von Karman's constant (0.4). The kinematic viscosity of air, υ, was assumed to be constant ($\approx 1.56 \times 10^{-5}\,\mathrm{m^2\,s^{-1}}$), so was the thermal diffusivity in air, D ($\approx 1.9 \times 10^{-5}\,\mathrm{m^2\,s^{-1}}$). The integral stability correction functions Ψ_h and Ψ_m for heat (h) and momentum (m), respectively, were taken from Businger et al. (1971) and Dyer (1974).

2.3 VOC measurements

2.3.1 PTR-ToF measurements

The PTR-ToF (Ionicon Analytik GmbH, Austria; Graus et al., 2010; Jordan et al., 2009) combines the soft ionization of a PTR source with the high mass resolution of a time of flight of mass spectrometer $\sim 4500\,\mathrm{m}/\Delta\,\mathrm{m}$ (determined as the full width at half maximum of the ion peak). The precise mass of a compound can be derived from the time of flight and the elemental composition can be calculated from the observed mass defect. Therefore the instrument can separate isobaric compounds; it cannot, however, distinguish between isomeric compounds, as it gives no information about the compound structure. The real-time measure of full spectra at 10 Hz allows for flux measurements with the eddy covariance technique.

The PTR-ToF was placed inside a container next to the measurement tower. Air from 32 m height was sampled through a 40 m long and 0.5 in wide (outer diameter;

o.d.) PDFE tube (hereafter referred to as common sampling line), which was pumped at 63 L min^{-1}. The pressure drop induced by the pumping was sufficient to prevent condensation in the sampling line outside of the container. Inside the air conditioned container, the inlet line was heated. The 3-d wind measurements were obtained with a frequency of 10 Hz 10 cm above the inlet.

The PTR-ToF was connected to the inlet line via a 3-way valve, from where a subsample of 0.5 L min^{-1} were pumped through a 1/8 in (o.d.) and 1/16 in (o.d.) capillary (together around 20 cm long) to the instrument. The PTR-ToF used a 30 mL min^{-1} flow for analysis, the remaining flow was discarded and served only as a by-pass flow in order to decrease the response time of the PTR-ToF and associated wall losses in the inlet capillaries. The drift tube was operated at 600 V and temperature of 60 °C. Together with a drift tube pressure of 2.3 mbar this resulted in an E_{PTR}/N ratio of 130 Td, where E_{PTR} is the electrical field strength and N is the gas number density. The instrument produced a time series of 22 days, with a 1.5 day break when the air-conditioning in the container failed.

2.3.2 Calibration and concentration calculation

The instrument background was measured one to three times per day. A small pump (N86KNE, KNF Neuberger) established a 1.4 L min^{-1} flow from the common sampling line to a custom made catalytic converter. This converter was heated to 350 °C and created VOC-free (zero-)air at ambient humidity. The zero air was connected to the second port of the three way valve and passed an overflow in order to achieve a constant zero air flow at a constant pressure (Fig. 2). The background (zero-air) measurements were used for the calculations of the concentrations as well as the determination of the limit of detection.

The instrument was calibrated every second week, i.e. a total of three times. A custom build calibration unit, which spiked zero air with the calibration gas, was inserted between the catalytic converter and the overflow (Fig. 2). The calibration gas (Apel Riemer Environmental Inc., USA) contained 16 different compounds with the mass range from 33 to 180 amu at known concentrations of around 1 ppm. The gas was diluted with zero air (calibration gas: 10 mL min^{-1}; zero air: 1.4 L min^{-1}) resulting in mixing ratios around 7 ppb. The sensitivities were calculated from the observed count rates of the zero air and the calibration gas measurements in the ppb range. For the VOCs that were not included in our calibration standard, we used average sensitivities for compound families C_xH_y (based on isoprene, benzene, toluene, o-xylene, trimethylbenzene, naphthalene, α-pinene combined with $C_6H_9^+$ fragment), $C_xH_yO_z$ (considering acetaldehyde, acrolein, acetone, 2-butanone) and $C_xH_yN_z$ (set to that of acetonitrile). The averaged sensitivities were: $C_xH_y = 13\,(\pm 1.7)$ ncps ppb^{-1}, $C_xH_yO_z = 19.1\,(\pm 1.3)$ ncps ppb^{-1} and $C_xH_yN_z = 18.1\,(\pm 1.3)$ ncps ppb^{-1}. The range given in the brackets is the standard deviation of the average sensitivities calculated for the compounds in each group from the calibrations. Normalized counts per second (ncps) have been corrected for pusher duty cycle losses and primary ion fluctuations (Herbig et al., 2009). The monoterpene sensitivities were derived from the α-pinene calibrations (in the calibration gas). For compounds included in the standard, the calibration implicitly accounts for the fragmentation pattern. For example, the signal at $C_5H_9^+$ (m/z 69.0699) relates to the protonated parent ion of isoprene and is scaled up to the total isoprene, although some isoprene fragments also show up at other masses. As a consequence it is important that fluxes at those fragments are excluded to avoid double-counting. The importance of this procedure is assessed in Sect. 3.1 below.

For compounds/fragments not included in the calibration standard, including those that could not be linked to a parent ion, the average sensitivities for the fragment families are applied as previously described. In this case the fragmentation pattern is not accounted for and all fragments have to be added up to arrive at the total flux, excluding those that could be associated with calibrated compounds.

For the data post processing the ToF Analyzer V2.45 software was used, which has been described in Müller et al. (2010, 2013). A peak list was created with the TofTools software (Junninen et al., 2010), by integrating the 10 Hz raw data for one hour and then fitting and identifying the different peaks. The measured mass peaks were identified by matching them with the calculated masses of different combinations of H, C, O, N and S atoms. The range of atoms allowed to appear in a compound was set from 0 to 50.

After peak fitting was performed on the 10 Hz data the output of the ToF analyzer were aggregated to provide 30 min concentration data in a three-step process: first, the 10 Hz data were averaged over 30 min. From these 30 min data the zero air measurements were subtracted, wherein values for the times between the zero air measurements were linearly interpolated. The resulting signals were then compared to the limit of detection $\mathrm{LOD} = 2\sigma_{\mathrm{zero}}$, where σ_{zero} is the standard deviation of the zero-air signal. To calculate the volume mixing ratios, all compounds above the LOD were divided by the measured or assigned sensitivity. Compounds with signals below the LOD were disregarded from the further analysis.

2.3.3 Flux calculations

Fluxes were derived using the eddy covariance method. In the EC, the flux is calculated using a discretized covariance:

$$\overline{w'c'} = \frac{1}{n}\sum_{i=1}^{n} w'(i-\lambda/\Delta t)c'(i), \tag{8}$$

where w' and $c'$are high frequency fluctuations of vertical wind and concentration, respectively, i the number of the measurement, n is the sum of all measurements during the flux averaging time (30 min in this study), Δt is the sampling interval and λ is the lag time caused by the sampling tubes (e.g. Kaimal and Finnigan, 1994).

In this study, vertical wind and VOC concentrations were both recorded at 10 Hz frequency. The compounds for which the flux was deemed detectable were identified with two different methods, which are termed the “classical method” (Taipale et al., 2010) and the “automated method” (Park et al., 2013).

The flux calculation procedure was the following:

first, the wind vector was 2-D-rotated using the method described by Kaimal and Finnigan, (1994). If the vertical rotation was more than 5°, the period was rejected from further analysis.

Block-averaging was used for the vertical wind measurements and the linear trend was removed from the concentration measurements.

Next, we calculated cross covariances between the vertical wind and the volume mixing ratios for every 30 min measurement period and determined a lag time by maximizing the smoothed cross covariance function from a lag time window of 0–5 s (classical approach, Taipale et al., 2010). For the automated approach, like in Park et al. (2014), a constant lag time was used for all compounds. This minimizes overestimations, which happen if the maximizing method is used for flux values close to the detection limit. The lag time was calculated from the averaged cross covariance function of isoprene and was 2.6 s. The individual 30 min lag times from the selected time window were also calculated to ensure that the lag time did not shift during the campaign.

Finally, the fluxes were filtered using a stationarity criteria introduced by Foken and Wichura, (1996): every 30 min period was divided into six 5 min sub-periods and VOC fluxes were calculated from both 5 and 30 min intervals. If the values differed more than 30 %, the period was disregarded from further analysis.

Next we assessed which compounds flux was above the limit of detection.

In the classical approach the cross covariance functions (CCFs) are checked manually for several different 30 min periods and it is determined if there is a clear maximum.

The automated method calculates fluxes as presented by Park et al. (2013). They used an automated flux searching routine, which calculated the average of absolute CCF. Therefore, a time window is chosen when good conditions for turbulence and high emissions are present. As in Park et al. (2013), a daily window from 10:00 to 16:00 (CET wintertime) was used in this study. The absolute values of the 30 min CCFs in this time window were averaged over the entire measurement period. From this averaged CCF a routine automatically finds the maximum value and compares it to a manually chosen noise level (3–10σ_{noise}, the standard deviation of the noise). The standard deviation is calculated from areas at the left and right border of the CCF spectra. The filtering of the data was done according to Park et al. (2013), where a 5° tilt angle and 70 % stationary criteria were used. The quality criteria disregarded 43 % of the data for the automated method and 43 % for the classical method. A comparison of the two methods is presented in Table 1.

For those compounds for which a flux could be detected, the uncertainty of the flux was calculated from the two 60 s time windows at the border of the CCFs for each 30 min flux value. The root mean square of each window was calculated and the results averaged. This follows the approach of Langford et al. (2015) and ensures that offsets (from zero) from the noise in the CCF tails are taken into account. For the diurnal net flux error it was assumed that the errors are independent, and the error was calculated with the Gaussian propagation of error. The independence assumption is not fully correct, as fluxes from different compounds are derived using the same vertical wind data.

For the calculation of the diurnal 30 min flux data, a trimmed mean function was used, which disregarded the lowest and highest 5 % of the data and then averages the remaining 90 % of the data. The flux data is not normally distributed and thereby this averaging method is will bias the result, but the positive aspects of limiting the influence of outliers were more important. The daily average was then calculated by averaging the diurnal data.

2.3.4 Spectral corrections

Due to the high frequency attenuation and low frequency cut-off, the measured EC flux underestimates the real flux (e.g. Horst, 1997; Moore, 1986). This attenuation is caused by the tubing, the sensor separation and the time-response of the instrument itself.

The effect of low-pass filtering can be quantified by the use of a transfer function. Formally the transfer function H_{wc} can be written as,

$$H_{wc}(f) = \frac{C_{wc}(f)}{\overline{w'c'}} \cdot \frac{C_{w\theta}(f)}{\overline{w'\theta'}}, \tag{9}$$

where C_{wc} and $C_{w\theta}$ are the cospectra of a scalar c and w, and potential temperature θ and w, respectively. $\overline{w'c'}$ and $\overline{w'\theta'}$ are "un-attenuated" turbulent fluxes of a scalar and temperature, respectively, and f is the frequency. A commonly used approximation for the first order transfer function is (Horst, 1997)

$$H_{wc} \approx [1 + (2\pi\tau f)^2]^{-1}, \tag{10}$$

where τ is a system response time.

In this study, we determined the high frequency attenuation using a method described by Horst (1997). In the method the attenuation factor α is calculated by the equation

$$\alpha = \frac{\overline{(w'c')_a}}{\overline{w'c'}} = \frac{1}{1 + \left(\frac{2\pi n_{\mathrm{m}} \tau \overline{u}}{z_{\mathrm{m}} - d}\right)^{\beta}}, \tag{11}$$

where z_{m} is the measurement height (32 m), d the zero displacement height ($d = 2/3 \times z_{\mathrm{c}}$, where z_{c} is the canopy height, 28 m), $\overline{u}$ the mean horizontal wind speed, $\overline{(w'c')_a}$ is the attenuated flux and $\overline{w'c'}$ is the real flux. For neutral and unstable stratification $(z_{\mathrm{m}} - d)/L \leq 0$, $\beta = 7/8$, $n_{\mathrm{m}} = 0.085$ and for stable stratification, $(z_{\mathrm{m}} - d)/L > 0$, $\beta = 1$, $n_{\mathrm{m}} = 2.0 - 1.915/[1 + 0.5(z_{\mathrm{m}} - d)/L]$.

We selected daytime (10:00–16:00 CET wintertime), unstable ($\overline{w'T'} > 0$) periods, and calculated cospectra of temperature, isoprene and water clusters for every 30 min interval. Response times of isoprene and water clusters were then derived by using

Eq. (10) and the median transfer functions (Eq. 9). After that, the flux losses were derived using the correction factor α^{-1} (Eq. 11) and the response time of the isoprene measurements (τ = 1.1 s; Fig. 3), which is similar to Rantala et al. (2014), where disjunct EC was utilized with a PTR-QMS. The correction factor α^{-1} was finally multiplied to each VOC flux value. On average this factor was 1.26.

2.3.5 Flux loss due to chemical degradation

The chemical degradation of different VOCs is dependent on their concentration, reaction rates and concentrations of oxidants (O_3, NO_3, OH). Therefore the proxy for OH concentration, $[OH]_{proxy}$, was calculated according to Peräkylä et al. (2014) and Petäjä et al. (2009):

$$[OH]_{proxy} = 5.62 \times 10^5 \times UVB^{0.62} \tag{12}$$

As the UVB radiation was not measured directly during the Bosco Fontana study, an upper limit calculation was made by using the tropospheric ultraviolet model 4.1 (TUV; Madronich, 1993; Madronich and Flocke, 1999). The model was used via the link http://cprm.acd.ucar.edu/Models/TUV/Interactive_TUV/, using the Pseudo-spherical discrete ordinate 4 streams radiation transfer model and an albedo of 0.1. The NO_3 concentration was calculated as described in Peräkylä et al. (2014) from the measured concentrations of NO_2 and O_3.

The influence of chemical degradation on the measured eddy covariance fluxes depends on the relative magnitude of the chemical lifetime of the measured compound and its transport time. The transport time is the time the compound needs to get from its emission point to the actual measure point, and it can be characterized by turbulent mixing time-scale. The effect is often assessed using the Damköhler number (Damköhler, 1940), which is the ratio of the mixing time-scale to the chemical lifetime. The smaller the Damköhler number is, the less influence the chemical degradation has on the flux. However, since both the transport time and the chemical lifetime are height dependent, a more accurate assessment of the loss is achieved by calculating the ratio of the flux at the measurement height (F) to the true surface emission (E) using a stochastic Lagrangian transport model (Rinne et al., 2012). In Bosco Fontana, the F/E for isoprene was 0.95–0.97, meaning that between 3 % and 5 % of the emissions are lost due to chemical degradation. For the monoterpenes (we used α-pinene), which have the lowest F/E ratio (shortest lifetime) of the measured flux compounds, the F/E was between 0.8 and 0.95. No corrections for the chemical degradation have been made in this manuscript.

2.4 Modelled MVK/MACR production

After having quantified the average fraction of the isoprene flux lost between point of emission and the measurement height, this section seeks to quantify the amount of MVK/MACR that is expected to be produced by an alternative approach, by integration of the chemical kinetic equation.

The chemical destruction of isoprene Q, in an air column below the measurement level can be calculated as

$$Q = \int_0^{z_m} \sum_i k_i \left[R_i\right] \left[C_5H_8\right] dz, \qquad (13)$$

where k_i is the rate constant, $[R_i]$ the concentration of reactant i, and $\left[C_5H_8\right]$ the concentration of isoprene. The integration is done from surface to the measurement height z_m. Even though $\left[C_5H_8\right]$ and $[R_i]$ are height dependent (Andronache et al., 1994; Hens et al., 2014), we assumed constant reactant and isoprene concentrations for the integration range in order to get an order of magnitude estimate. We estimated the chemical destruction for two ranges: from the ground level 0 to the measurement height and from the notional height $(d + z_0)$ to the measurement height. The angle brackets ⟨⟩ indicate that the values are constant:

$$Q = k_i \langle [R_i] \rangle \langle [C_5H_8] \rangle z_m \tag{14}$$

$$Q = k_i \langle [R_i] \rangle \langle [C_5H_8] \rangle (z_m - d - z_0) \tag{15}$$

In order to estimate the yield of methyl vinyl ketone (MVK) and methacrolein (MACR) from isoprene, we selected the isoprene chemistry mechanism from the Master Chemical Mechanism (MCM) v3.2 (Jenkin et al., 1997; Saunders et al., 2003), via website http://mcm.leeds.ac.uk/MCM/. The concentrations of MVK and MACR were calculated using the Kinetic PreProcessor (Damian et al., 2002) coupled to the box model MALTE-BOX (Boy et al., 2013). The simulation was executed using an initial concentration of isoprene (5.33×10^{10} # cm^{-3}; measured) and constant concentrations of OH (1×10^6 # cm^{-3}; calculated), O_3 (2×10^{12} # cm^{-3}; measured), NO (3.5×10^9 # cm^{-3}; measured), NO_2 (8×10^{10} # cm^{-3}; measured), SO_2 (1×10^9 # cm^{-3}; estimated) and CO (3.5×10^{12} # cm^{-3}; estimated). The temperature was further kept constant to a value of 303 K, while the start of the simulation was assumed to be at noon (local time). By dividing the initial concentration of isoprene by the summed maximum concentration of MVK and MACR, we estimate that the summed yield of MVK and MACR from oxidized isoprene is 0.35. A sensitivity test showed that the MVK/MACR yield response to a change in temperature and SO_2 concentration is minor. For CO, a concentration change to 5×10^{13} # cm^{-3} results in a 5 % lower yield. Due to the high NO_x concentration in Bosco Fontana, the reaction way via isoprene hydroxy hydroperoxides (ISOPOOH) does not form MVK/MACR.

3 Results and discussion

3.1 Comparison of procedures to identify detectable fluxes

In the following chapter the data from 22 days of flux measurements are used by different analysis routines, and the results are compared. Negative fluxes are called deposition, as it is not possible to differentiate between deposition and other sink terms such as chemical losses below the measurement height; the positive fluxes are called emissions. The diurnal cycles of the ten most emitted compounds for each calculation method are shown in Fig. 4. The signals of the remaining masses with detectable flux quantified by both methods are summed up and plotted as “other”. The 24 h average flux of the different compounds and different methods is shown in Table 2.

The average total deposition of the VOCs detected with the three different methods was −0.4 (± 0.1) $\text{nmol}\,\text{m}^{-2}\,\text{s}^{-1}$ and the average total emission was 9.5 (±1.0) $\text{nmol}\,\text{m}^{-2}\,\text{s}^{-1}$. The classical method identified the smallest number of compounds (5), accounting for the lowest total emission (8.52 $\text{nmol}\,\text{m}^{-2}\,\text{s}^{-1}$) and also the lowest total deposition (−0.28 $\text{nmol}\,\text{m}^{-2}\,\text{s}^{-1}$). The only compound with a flux that was deemed quantifiable by the classical method but not by the others was $C_5H_9O_2^+$ (protonated), which contributed by 0.5 % to the total deposition and by 0.2 % to the total emission.

The automated method with a 10 σ_{noise} threshold found most compounds with detectable flux (19) and had the highest total emission (10.6 $\text{nmol}\,\text{m}^{-2}\,\text{s}^{-1}$). The main additional masses with detectable flux were acetone, acetaldehyde and acetic acid. However, several of the compounds were recognized as fragments, water-clusters or charge transfer peaks of compounds included in the calibration standard, especially $C_3H_5^+$, $C_6H_9^+$, $C_2H_3O^+$ and the $C_1H_7O_2^+$. This can lead to an overestimation of the emission or deposition, due to double-counting (see Sect. 2.3.2). Furthermore, the diurnal pattern of water-cluster ionized compounds will be heavily influenced by the amount of $H_3O^+ \cdot H_2O$, which is dependent on the RH (as well as several instrumental settings, which, however, did not change during the measurements). In this study, this was especially important, as over 60 % of the total emission were caused by isoprene, therefore even minor fragments of isoprene can have a considerable impact on the net flux. Overall, 7.3 % of the total deposition and 9.6 % of the total emission were caused by fragments, clusters and charge transfer peaks of calibrated compounds. When the masses with detectable flux were filtered for known fragments, the total emission decreased by 10 % and the compounds with flux decreased to 12. It is important to keep in mind that the absolute flux-values of each compound for the automated method and the automated method with compound filter are the same. The filtering only changes the relative flux (due to the change of the net flux).

Figure 5 shows the diurnal variation of the net flux for the different approaches. The difference in the net flux between a 3 σ_{noise} threshold and a $10\sigma_{\text{noise}}$ threshold is less than 1.6 $\text{nmol}\,\text{m}^{-2}\,\text{s}^{-1}$. The major difference lies in the number of masses that are found to contribute to the total VOC flux: 42 ($3\sigma_{\text{noise}}$), 35 ($4\sigma_{\text{noise}}$), 28 ($5\sigma_{\text{noise}}$), 24 ($6\sigma_{\text{noise}}$), 23 ($7\sigma_{\text{noise}}$), 22 ($8\sigma_{\text{noise}}$), 20 ($9\sigma_{\text{noise}}$), 19 ($10\sigma_{\text{noise}}$).

The classical method is rather labor intensive, because the CCF must be checked for many different mass peaks (> 150, depending on the environment where the measurements are recorded), for several different times of the campaign (overall well over 1000 CCFs). Another weakness is that the definition of a "clear maxima" is not objective and depends on the person who is working with the data. A positive aspect is that during the manual evaluation of the data possible problems or analysis faults can be detected more easily.

Compared to the classical method, the automated method gives a fast and objective result, but the σ_{noise} threshold can vary, as the standard deviation of the noise can be reduced by taking its absolute value. The reduction of the standard deviation takes place if the signal, which is used for the error calculation, is around zero and, therefore, varies between negative and positive values. If there is some offset, so that the signal is just positive or just negative inside the error areas, using absolute values does not influence the value of σ_{noise}.

As shown, when combining calibrated and uncalibrated data, double-counting of fragments can lead to an overestimation of the flux and should therefore be filtered. In the remaining paper, all mentioned flux values will be calculated using the automated method with compound filter and all times will be CET wintertime (UTC +1 h).

3.2 Emission of terpenoids

The most abundant compound emitted by the Bosco Fontana forest was isoprene (protonated formula: $C_5H_9^+$), comprising over 65 % of the measured total emission. It has a clear diurnal cycle which follows the radiation. The maximum emission (diurnal) at 20.6 $\text{nmol}\,\text{m}^{-2}\,\text{s}^{-1}$ occurred just after midday. Figure 6b shows the wind rose for the isoprene flux. There are more isoprene emitting plants to the west of the site, indicated by the highest fluxes coming from this direction. Indeed, Acton et al. (2015) found that taking the contribution of the strong emitters in this wind sector into account improved the correlation between predicted and measured isoprene fluxes. Similar behavior can be seen from the wind rose of the isoprene concentrations, although the extent of the forest is smaller towards SW, providing less opportunity for isoprene to accumulate during advection. From 21:00 to 05:00 CET the emissions stayed below 0.1 $\text{nmol}\,\text{m}^{-2}\,\text{s}^{-1}$. The main sink of isoprene is oxidation due to reactions with OH during daytime. The calculated isoprene lifetime for daytime conditions in Bosco Fontana is 2.2 h.

The fast oxidation, together with the relatively small extent of the woodland in a mixed agricultural landscape with relatively low isoprene emissions, explains why the diurnal concentration maximum of isoprene was only 2.8 ppb, even though the isoprene emission is dominating all other measured VOCs. Its daily average concentration was 1.3 ppb. The emission factors of isoprene and monoterpenes in Bosco Fontana, as well as the as the relative importance of pool and de novo emissions, are discussed in Acton et al. (2015). Isoprene's major source globally are forests (Guenther et al., 1995), oaks are known for being isoprene emitters (Rasmussen, 1970) and dominate European isoprene emissions. Potosnak et al. (2014) measured a maximum isoprene emission of 217 $\text{nmol}\,\text{m}^{-2}\,\text{s}^{-1}$ over an oak-dominated temperate forest in central Missouri.

2-methyl-3-buten-2-ol (MBO) can dehydrate in the proton transfer reaction and form isoprene (Fall et al., 2001, de Gouw and Warneke, 2006; Kaser et al., 2013). The influence on the isoprene signal depends on the MBO concentration and the settings of the PTR-ToF. The influence of MBO to the isoprene signal in Bosco Fontana should be minor, as the major tree species are known to be isoprene or monoterpene emitter (Konig et al., 1995; Harley et al., 1999; Rosenstiel et al., 2002) as confirmed by the more specific leaf level measurements of Acton et al. (2015). However, a possible MBO source could be the understory of the forest.

In Bosco Fontana monoterpenes have been the fifth most emitted "compound group". With the PTR-TOF it is only possible to measure the sum of all monoterpenes, which had a maximum emission of 0.7 $\mathrm{nmol\,m^{-2}\,s^{-1}}$. Leaf-level measurements at Bosco Fontana presented by Acton et al. (2015) found the largest monoterpene emissions to be limonene originating from *Carpinus betulus* and *Corylus avellana* and to some extent *Comus sanguinea*, augmented with smaller emissions of α-pinene from *Q. robur* and *Acer campestre*, and β-pinene from *A. campestre* and *C. betulus*. Figure 6b shows the normalized wind rose of the monoterpenes emissions (independent of the frequency of wind directions). The measurement site is very homogeneous, as no wind direction dependency on the monoterpenes flux was detected. This also holds for the monoterpene concentrations.

3.3 MVK/MACR and their sources

MVK and MACR have the same elemental composition (protonated formula: $C_4H_7O^+$), and cannot be separated with our instrument settings. In Bosco Fontana, 3 % of the total emissions were due to MVK/MACR, which are both oxidation products of isoprene. To give an estimate of how much of the MVK/MACR flux is likely to have originated from atmospheric oxidation of isoprene below the measurement level z_m, we used two methods to estimate the flux divergence. The oxidation of isoprene is dominated by the reaction with the OH radical. The daytime maximum isoprene oxidation rates between ground level and measurement height are around 0.61 $\mathrm{nmol\,m^{-2}\,s^{-1}}$ (Eq. 14) and if the lower limit is the notional height 0.24 $\mathrm{nmol\,m^{-2}\,s^{-1}}$ (Eq. 15). However, the result of the integration (Eq. 13) varies considerably depending on the integration domain and the assumed profiles.

Another approach to estimate the chemical degradation is to use the look-up tables for Flux-to-Surface-Exchange (F/E) ratios created using a stochastic Lagrangian transport model by Rinne et al. (2012). For the F/E ratio we use typical daytime values of friction velocity and chemical lifetime of isoprene. Depending on the assumed oxidant profile and leaf area index, we have F/E ratios ranging between 0.97–0.95. Multiplying the isoprene emission by F/E ratio leads to the oxidation rates between 0.6–1.0 $\mathrm{nmol\,m^{-2}\,s^{-1}}$.

According to our calculations (Sect. 2.4), 35 % of the oxidized isoprene molecules will create MVK or MACR molecules (for midday conditions). The scatterplot between the concentration of isoprene and the MVK/MACR flux (Fig. 7a) shows a correlation coefficient of 0.65. If we compare the measured MVK/MACR flux to the calculated source of MVK/MACR by the oxidation of isoprene below the measurement height, we get a correlation coefficient of 0.81 (Fig. 7b). The correlation however, does not imply causality. The biogenic VOC emissions and concentrations are light dependent, as well as the concentration of OH radicals which may lead to correlations where causality does not exist.

The one hour data in both plots was separated into day and night by using a 200 $\mathrm{\mu mol\,m^{-2}}$ photo active radiation threshold. Then the $\frac{y}{x}$ ratios of Fig. 7a and b daytime data were used to calculate the median and percentile ratios. From the 25 and 75 % iles ratios we estimated the influence of the oxidation of isoprene to the measured MVK/MACR flux. If Eq. (14) is used to calculate this influence the oxidation products of isoprene causes between 11 and 27 % of the MVK/MACR flux. If Eq. (15) is used, the contribution of isoprene to the MVK/MACR flux is between 4 and 11 %.

Comparing the results of the F/E calculations with the maximum diurnal MVK/MACR flux of 1.3 $\mathrm{nmol\,m^{-2}\,s^{-1}}$ shows that a contribution of 16 to 27 % of the MVK/MACR flux may originate from atmospheric chemistry. Overall the oxidation of isoprene may have an important influence (4 to 27 %) on the MVK/MACR flux, but fails to explain it fully.

Fluxes can also originate from direct MVK/MACR emissions from the plant as shown by Jardine et al. (2012). Part of the MVK/MACR concentration and fluxes may also be misattributed fragments from higher oxygenated hydrocarbons, which get destroyed inside the instrument (Liu et al., 2013; Rivera-Rios et al., 2014). MVK and MACR have also been found to be formed from the decomposition of hydroxyl hydroperoxides (ISOPOOH) in the PTR-MS inlet. However, ISPOOH reacts readily with NO and its concentration in polluted environments such as the Po Valley would therefore be expected to be very low, and consequently this artefact can be ruled out at this location.

In general, a comprehensive theory of MVK/MACR emission and deposition is lacking, while in some environments (especially in the tropics) MVK/MACR are found to deposit fast, approaching the maximum rate permitted by turbulence (i.e. with a small canopy uptake resistance; cf Misztal et al., 2011, and references therein), whilst in other environments like at Bosco Fontana emissions are observed.

3.4 Emission of oxygenated VOCs

The second-most emitted compound was methanol (protonated formula: CH_5O^+), whose net flux started later in the day than the rest of the VOC emissions. It contributed with 14 % to the total emission (maximum emission at 14:30 CET with $4.4\,\mathrm{nmol\,m^{-2}\,s^{-1}}$). Methanol is mostly emitted by plants e.g. by the plant growth metabolism (Wohlfahrt et al., 2015). From the wind rose in Fig. 6b it can be seen that the highest methanol emissions originated from the west.

The third most emitted compound was acetone, which had a diurnal maximum emission at 11:30 CET, at $1.0\,\mathrm{nmol\,m^{-2}\,s^{-1}}$. Its daily average contributed with over 3 % to the total emission (daily average). It has the same elemental composition as propanal. However, the contribution of propanal is normally less than 10 % to the signal (de Gouw and Warneke, 2006). Acetone sources are ubiquitous: it can be emitted from several plants and trees (Geron et al., 2002; Fall, 1999), emitted from anthropogenic processes (Singh et al., 1994) or produced through secondary photochemical production (Goldstein et al., 2000).

Title Page
Abstract | Introduction
Conclusions | References
Tables | Figures
◀| |▶
◀ ▶
Back | Close
Full Screen / Esc
Printer-friendly Version
Interactive Discussion

The emission of acetaldehyde peaked around 11:30 CET at 0.7 nmol m^{-2} s^{-1}. It is a hazardous air pollutant (EPA, 1994), and plays an important role in the formation of ozone, HO_x radicals (Singh et al., 1995) and PAN (Roberts, 1990).

The maximum emission of acetic acid was at 11:30 CET at 0.5 nmol m^{-2} s^{-1}. Its sources are manifold: it is emitted by soil and vegetation, from animal husbandry, it can be produced photochemically and it is also a combustion marker for biomass and fossil fuels (Chebbi et al., 1996).

Other reported sources of carbonyls are conifers (e.g. Janson et al., 1999; Rinne et al., 2007) and decaying vegetation (e.g. de Gouw et al., 2000; Karl et al., 2001; Warneke et al., 2002). The remaining compounds each contributed less than 1 % to the total emission.

3.5 VOC deposition

For wet or dry deposition, the ambient concentration of the deposited compound plays an important role. Figure 8 shows the total VOC concentration detected by the PTR-ToF and its diurnal behavior. The highest total VOC concentrations occur during the night, when the planetary boundary layer is shallower and the volume, into which the VOCs are emitted, is smaller. However, concentrations of biogenic VOCs (e.g. isoprene, monoterpenes) were much smaller during the night, reflecting a combination of smaller emissions and influences from air from outside the forest; the footprint for concentration measurements is much larger than the Bosco Fontana forest. By contrast long-lived compounds, which can also be of anthropogenic origin, increase in concentration at nights. One of them, methanol, showed the highest concentration and highest deposition (Table 3). The wind rose for the methanol concentration is shown in Fig. 6b. Highest concentrations were measured when the wind direction was northeast and southwest. The deposition of methanol generally lasted from 01:00 to 08:00 CET. During this period also highest concentrations were measured. It seems that methanol concentrations were considerably affected by horizontal transport or secondary production. Since the largest concentrations were measured when the wind speed was below 2 m s^{-1}, major source for this compound must be located outside the forest but close to the measurement site. Overall methanol accounted for 83 % to the total deposition observed. The main sinks are reactions with OH and dry and wet deposition, which restrict the atmospheric lifetime of methanol to seven days (Jacob et al., 2005). The methanol deposition in the early mornings could be due to wet deposition on dew. The deposition of methanol has been observed in other studies (e.g. Holzinger et al., 2001; Riemer et al., 1998 and Goldan et al., 1995; Wohlfahrt et al., 2015). Laffineur et al. (2012) observed very large methanol uptake, which they suggest to be caused by adsorption/desorption to water films. In Fig. 9 the ambient temperature and the dew point temperature are shown. The colored background in the figure marks when the methanol deposition occurred (as can be seen in the diurnal flux plot in Fig. 4). The deposition occurs when the surface temperature was closest to the dew point.

Acetic acid showed the second highest deposition, which contributed with more than 10 % to the total deposition. It has the third highest concentration (Table 3) and a lifetime of 1.7 days in the boundary layer (Paulot et al., 2011).

Next is acetone, which accounted for 2.3 % to the total deposition. It has the second highest concentration (Table 3) and the tropospheric lifetime is reported to be 15 days (Jacob et al., 2002). Minor deposition fluxes were calculated for MVK/MACR (1.1 %), which can be affected by fragmentation (Sect. 3.4; Rivera-Rios et al., 2014), and methyl acetate (1.1 %). The remaining compounds each contributed less than 1 % to the total deposition.

4 Conclusions

During the Bosco Fontana campaign a total of twelve compounds with detectable flux were identified, for which a flux could be quantified, by using the automated method with compound filter. These compounds were dominated by isoprene, which comprised 65 % of the total emission. We estimated the influence of the atmospheric oxidation of isoprene to the MVK/MACR flux. The calculated chemical production can explain up to 27 % of the MVK/MACR flux. Thus, the major part of the MVK/MACR flux remains unaccounted for by this source.

The deposition of methanol was assumed to be due to dry deposition to leaf water layers (incl. dew) as deposition coincided with the calculated ratios of dew point to surface temperature approaching unity.

Using the data measured in Bosco Fontana, we compared the classical method to determine which compounds showed significant fluxes, with an automated approach ($10\sigma_{\text{noise}}$). The results of the methods differed by 20 % for the total emission and 41 % for the total deposition. This indicates that 80 % of the flux was covered by the classical method. The flux compounds identified ranged from 5 (classical method) to 48 (automated method with $3\sigma_{\text{noise}}$). With the automated method with compound filter ($10\sigma_{\text{noise}}$) 12 flux compounds were identified. We recommend the automated method with compound filter, which combines the fast analysis and better flux detection, without the overestimation due to double counting.

Acknowledgements. We would like to thank Markus Müller for providing the PTR-ToF Data Analyzer and Heikki Junninen and the tofTools team for providing the tofTools. We are further grateful to our colleagues from the Catholic University Brescia, and in particular Giacomo Gerosa and Angelo Finco, for the preparation of the tower and measurement infrastructure and to the Corpo Forestale dello Stato for access to the site. Thanks to all participants of the Bosco Fontana campaign, especially to Joe Acton for discussing and comparing the fluxes measured with PTR-QMS and PTR-ToF, to Ben Langford and Mhairi Coyle for helping with the installation on the tower. The data for the annual mean temperature and precipitation (UDel_AirT_Precip) was provided by the NOAA/OAR/ESRL PSD, Boulder, Colorado, USA, from their Web site at http://www.esrl.noaa.gov/psd/.

This research received funding from the EC Seventh Framework Programme (Collaborative projects “ECLAIRE”, grant no. 282910, and “PEGASOS”, grant no. 265148) and from the Academy of Finland Centre of Excellence program (project number 272041).

References

Acton, W. J. F., Schallhart, S., Langford, B., Valach, A., Rantala, P., Fares, S., Carriero, G., Tillmann, R., Tomlinson, S. J., Dragosits, Gianelle, D., U., Hewitt, C. N., and Nemitz, E.: Canopy-scale flux measurements and bottom-up emission estimates of volatile organic compounds from a mixed oak and hornbeam forest in northern Italy, submitted to Atmos. Chem. Phys Discuss., 2015.

Andronache, C., Chameides, W. L., Rodgers, M. O., Martinez, J., Zimmerman, P., and Greenberg, J.: Vertical distribution of isoprene in the lower boundary layer of the rural and urban southern United States, J. Geophys. Res., 99, 16989–16999, doi:10.1029/94JD01027, 1994.

Bloss, C., Wagner, V., Bonzanini, A., Jenkin, M. E., Wirtz, K., Martin-Reviejo, M., and Pilling, M. J.: Evaluation of detailed aromatic mechanisms (MCMv3 and MCMv3.1) against environmental chamber data, Atmos. Chem. Phys., 5, 623–639, doi:10.5194/acp-5-623-2005, 2005.

Boy, M., Mogensen, D., Smolander, S., Zhou, L., Nieminen, T., Paasonen, P., Plass-Dülmer, C., Sipilä, M., Petäjä, T., Mauldin, L., Berresheim, H., and Kulmala, M.: Oxidation of SO_2 by stabilized Criegee intermediate (sCI) radicals as a crucial source for atmospheric sulfuric acid concentrations, Atmos. Chem. Phys., 13, 3865–3879, doi:10.5194/acp-13-3865-2013, 2013.

Businger, J. A. and Oncley, S. P.: Flux measurement with conditional sampling, J. Atmos. Ocean. Tech., 7, 349–352, 1990.

Businger, J. A., Wyngaard, J. C., Izumi, Y., and Bradley, E. F.: Flux–profile relationships in the atmospheric surface layer, J. Atmos. Sci., 28, 181–189, 1971.

Chebbi, A. and Carlier, P.: Carboxylic acids in the troposphere, occurrence, sources, and sinks: a review, Atmos. Environ., 30, 4233–4249, ISSN 1352-2310, doi:10.1016/1352-2310(96)00102-1, 1996.

Dalponte, M., Bruzzone, L., and Gianelle, D.: Fusion of hyperspectral and LIDAR remote sensing data for classification of complex forest areas, Geoscience and Remote Sensing, 46, 1416–1427, 2008.

Damian, V., Sandu, A., Damian, M., Potra, F., and Carmichael, G. R.: The kinetic preprocessor KPP – a software environment for solving chemical kinetics, Comput. Chem. Eng., 26, 567–1579, 2002.

Damköhler, G.: Der Einfluss der Turbulenz auf die Flammengeschwindigkeit in Gasgemischen, Z. Elktrochem. Angew. P., 46, 601–626, 1940.

de Gouw, J. A. and Warneke, C.: Measurements of volatile organic compounds in the earth's atmosphere using proton-transfer-reaction mass spectrometry, Mass Spectrom. Rev., 26, 223–257, doi:10.1002/mas.20119, 2006.

de Gouw, J. A., Howard, C. J., Custer, T. G., Baker, B. M., and Fall, R.: Proton-transfer chemical-ionization mass spectrometry allows real-time analysis of volatile organic compounds released from cutting and drying of crops, Environ. Sci. Technol., 34, 2640–2648, 2000.

Derwent, R. G., Jenkin, M. E., Saunders, S. M., Pilling, M. J., Simmonds, P. G., Passant, N. R., Dollard, G. J., Dumitrean, P., and Kent, A.: Photochemical ozone formation in north west Europe and its control, Atmos. Environ., 37, 1983–1991, 2003.

Dolman, A. J.: Estimates of roughness length and zero plane displacement for a foliated and non-foliated oak canopy, Agr. Forest Meteorol., 36, 241–248, 1986.

Dyer, A. J.: A review of flux–profile relationships, Bound.-Lay. Meteorol., 7, 363–372, 1974.

EPA: Chemical Summary for Acetaldehyde, EPA 749-F-94-003a, Office of Pollution Prevention and Toxics, available at: http://onlinelibrary.wiley.com/doi/10.1002/9781118747926.app1/pdf (last access: 13 October 2015), 1994.

Fall, R.: Reactive Hydrocarbons in the Atmosphere, Academic Press, San Diego, USA, 41–96, 1999.

Fall, R., Karl, T., Jordan, A., and Lindinger, W.: Biogenic C5 VOCs: release from leaves after freeze–thaw wounding and occurrence in air at a high mountain observatory, Atmos. Environ., 35, 3905–3916, 2001.

Fehsenfeld, F., Calvert, J., Fall, R., Goldan, P., Guenther, A. B., Hewitt, C. N., Lamb, B., Liu, S., Trainer, M., Westberg, H., and Zimmerman, P.: Emissions of volatile organic compounds from vegetation and the implications for atmospheric chemistry, Global Biogeochem. Cy., 6, 389–430, 1992.

Foken, T. and Wichura, B.: Tools for quality assessment of surface-based flux measurements, Agr. Forest Meteorol., 78, 83–105, 1996.

Fuentes, J. D., Wang, D., Neumann, H. H., Gillespie, T. J., Den Hartog, G., and Dann, T. F.: Ambient biogenic hydrocarbons and isoprene emissions from a mixed deciduous forest, J. Atmos. Chem., 25, 67–95, 1996.

Fuentes, J. D., Gu, L., Lerdau, M., Atkinson, R., Baldocchi, D., Bottenheim, J. W., Ciccioli, P., Lamb, B., Geron, C., Guenther, A. B., Sharkey, T. D., and Stockwell, W.: Biogenic hydrocarbons in the atmospheric boundary layer: a review, B. Am. Meteorol. Soc., 81, 1537–1575, 2000.

Garland, J. A.: Dry deposition of sulfur-dioxide to land and water surfaces, P. Roy. Soc. A-Math. Phy., 354, 245–268, 1977.

Geron, C., Guenther, A. B., Greenberg, J., Loescher, H. W., Clark, D., and Baker, B.: Biogenic volatile organic compound emissions from a lowland tropical wet forest in Costa Rica, Atmos. Environ., 36, 3793–3802, ISSN 1352-2310, 2002.

Goldan, P. D., Kuster, W. C., Fehsenfeld, F. C., and Montzka, S. A.: Hydrocarbon measurements in the southeastern United States: the Rural Oxidants in the Southern Environment (ROSE) Program 1990, J. Geophys. Res., 100, 25945–25963, doi:10.1029/95JD02607, 1995.

Goldstein, A. and Schade, G. W.: Quantifying biogenic and anthropogenic contributions to acetone mixing ratios in a rural environment, Atmos. Environ., 34, 4997–5006, 2000.

Graus, M., Müller, M., and Hansel, A.: High resolution PTR-TOF: quantificationand formula confirmation of VOC in real time, J. Am. Soc. Mass Spectr., 21, 1037–1044, 2010.

Guenther, A. B., Hewitt, C. N., Erickson, D., Fall, R., Geron, C., Graedel, T., Harley, P., Klinger, L., Lerdau, M., McKay, W. A., Pierce, T., Scholes, B., Steinbrecher, R., Tallamraju, R., Taylor, J., and Zimmerman, P.: A global model of natural volatile organic compound emissions, J. Geophys. Res., 100, 8873–8892, doi:10.1029/94JD02950, 1995.

Guenther, A. B., Greenberg, J., Harley, P., Helmig, D., Klinger, L., Vierling, L., Zimmerman, P., and Geron, C.: Leaf, branch, stand and landscape scale measurements of volatile organic compound fluxes from U.S. woodlands, Tree Physiol., 16, 17–24 doi:10.1093/treephys/16.1-2.17, 1996.

Guenther, A. B., Jiang, X., Heald, C. L., Sakulyanontvittaya, T., Duhl, T., Emmons, L. K., and Wang, X.: The Model of Emissions of Gases and Aerosols from Nature version 2.1 (MEGAN2.1): an extended and updated framework for modeling biogenic emissions, Geosci. Model Dev., 5, 1471–1492, doi:10.5194/gmd-5-1471-2012, 2012.

Harley, P. C., Monson, R. K., and Lerdau, M. T.: Ecological and evolutionary aspects of isoprene emission from plants, Oecologia, 118, 109–123, 1999.

Hens, K., Novelli, A., Martinez, M., Auld, J., Axinte, R., Bohn, B., Fischer, H., Keronen, P., Kubistin, D., Nölscher, A. C., Oswald, R., Paasonen, P., Petäjä, T., Regelin, E., Sander, R., Sinha, V., Sipilä, M., Taraborrelli, D., Tatum Ernest, C., Williams, J., Lelieveld, J., and Harder, H.: Observation and modelling of HO_x radicals in a boreal forest, Atmos. Chem. Phys., 14, 8723–8747, doi:10.5194/acp-14-8723-2014, 2014.

Herbig, J., Müller, M., Schallhart, S., Titzmann, T., Graus, M., and Hansel, A.: On-line breath analysis with PTR-TOF, Journal of Breath Research, 3, 027004, doi:10.1088/1752-7155/3/2/027004, 2009.

Holzinger, R., Jordan, A., Hansel, A., and Lindinger, W.: Methanol measurements in the lower troposphere near Innsbruck (047°16′ N; 011°24′ E), Austria, Atmos. Environ., 35, 2525–2532, 2001.

Horst, T. W.: A simple formula for attenuation of eddy fluxes measured with first-order-response scalar sensors, Bound.-Lay. Meteorol., 82, 219–233, 1997.

Jacob, D. J., Field, B. D., Jin, E. M., Bey, I., Li, Q., Logan, J. A., Yantosca, R. M., and Singh, H. B.: Atmospheric budget of acetone, J. Geophys. Res.-Atmos., 107, 4100, doi:10.1029/2001JD000694, 2002.

Jacob, D. J., Field, B. D., Li, Q., Blake, D. R., de Gouw, J., Warneke, C., Hansel, A., Wisthaler, A., Singh, H. B., and Guenther, A. B.: Global budget of methanol: constraints from atmospheric observations, J. Geophys. Res., 110, D08303, doi:10.1029/2004JD005172, 2005.

Janson, R. and De Serves, C., and Romero, R.: Emission of isoprene and carbonyl compounds from a boreal forest and wetland in Sweden, Agr. Forest Meteorol., 98, 671–681, 1999.

Jardine, K. J., Monson, R. K., Abrell, L., Saleska, S. R., Arneth, A., Jardine, A., Ishida, F. Y., Serrano, A. M. Y., Artaxo, P., Karl, T., Fares, S., Goldstein, A., Loreto, F., and Huxman, T.: Within-plant isoprene oxidation confirmed by direct emissions of oxidation products methyl vinyl ketone and methacrolein, Glob. Change Biol., 18, 973–984, doi:10.1111/j.1365-2486.2011.02610.x, 2012.

Jenkin, M. E., Saunders, S. M., and Pilling, M. J.: The tropospheric degradation of volatile organic compounds: a protocol for mechanism development, Atmos. Environ., 31, 81–104, 1997.

Jordan, A., Haidacher, S., Hanel, G., Hartungen, E., Märk, L., Seehauser, H., Schottkowsky, R., Sulzer, P., and Märk, T. D.: A high resolution and high sensitivity proton-transfer-reaction time-of-flight mass spectrometer (PTR-TOF-MS), Int. J. Mass Spectrom., 286, 122–128, 2009.

Junninen, H., Ehn, M., Petäjä, T., Luosujärvi, L., Kotiaho, T., Kostiainen, R., Rohner, U., Gonin, M., Fuhrer, K., Kulmala, M., and Worsnop, D. R.: A high-resolution mass spectrometer to measure atmospheric ion composition, Atmos. Meas. Tech., 3, 1039–1053, doi:10.5194/amt-3-1039-2010, 2010.

Kaimal, J. C. and Finnigan, J. J.: Atmospheric Boundary Layer Flows: Their Structure and Measurement, Oxford University Press, New York, USA, 1994.

Karl, T., Guenther, A. B., Jordan, A., Fall, R., and Lindinger, W.: Eddy covariance measurement of biogenic oxygenated VOC emissions from hay harvesting, Atmos. Environ., 35, 491–495, doi:10.1016/S1352-2310(00)00405-2, 2001.

Kaser, L., Karl, T., Guenther, A., Graus, M., Schnitzhofer, R., Turnipseed, A., Fischer, L., Harley, P., Madronich, M., Gochis, D., Keutsch, F. N., and Hansel, A.: Undisturbed and disturbed above canopy ponderosa pine emissions: PTR-TOF-MS measurements and MEGAN 2.1 model results, Atmos. Chem. Phys., 13, 11935–11947, doi:10.5194/acp-13-11935-2013, 2013.

Kesselmeier, J. and Staudt, M.: Biogenic volatile organic compounds (VOC): an overview on emission, physiology and ecology, J. Atmos. Chem., 33, 23–88, 1999.

König, G., Brunda, M., Puxbaum, H., Hewitt, C. N., Duckham, S. C., and Rudolph, J.: Relative contribution of oxygenated hydrocarbons to the total biogenic VOC emissions of selected mid-European agricultural and natural plant species, Atmos. Environ., 29, 861–874, 1995.

Kulmala, M., Toivonen, A., Mäkelä J., and Laaksonen, A.: Analysis of the growth of nucleation mode particles observed in boreal forest, Tellus B, 50, 449–462, 1998.

Laffineur, Q., Aubinet, M., Schoon, N., Amelynck, C., Müller, J.-F., Dewulf, J., Van Langenhove, H., Steppe, K., and Heinesch, B.: Abiotic and biotic control of methanol exchanges in a temperate mixed forest, Atmos. Chem. Phys., 12, 577–590, doi:10.5194/acp-12-577-2012, 2012.

Lamb, B., Westberg, H., and Allwine, G.: Biogenic hydrocarbon emissions from decidous and coniferous trees in the United States, J. Geophys. Res., 90, 2380–2390, 1985.

Langford, B., Acton, W., Ammann, C., Valach, A., and Nemitz, E.: Eddy-covariance data with low signal-to-noise ratio: time-lag determination, uncertainties and limit of detection, Atmos. Meas. Tech. Discuss., 8, 2913–2955, doi:10.5194/amtd-8-2913-2015, 2015.

Lawrence, M. G: The relationship between relative humidity and the dewpoint temperature in moist air: a simple conversion and applications, B. Am. Meteorol. Soc., 86, 225–233, doi:10.1175/BAMS-86-2-225, 2005.

Liu, Y. J., Herdlinger-Blatt, I., McKinney, K. A., and Martin, S. T.: Production of methyl vinyl ketone and methacrolein via the hydroperoxyl pathway of isoprene oxidation, Atmos. Chem. Phys., 13, 5715–5730, doi:10.5194/acp-13-5715-2013, 2013.

Madronich, S.: UV radiation in the natural and perturbed atmosphere, in: Environmental Effects of UV (Ultraviolet) Radiation, CRC Press, Boca Raton, USA, 17–69, 1993.

Madronich, S. and Flocke, S.: The role of solar radiation in atmospheric chemistry, in: The Handbook of Environmental Chemistry, Vol. 2, Springer, Berlin, Germany, 1–26, 1999.

Misztal, P. K., Nemitz, E., Langford, B., Di Marco, C. F., Phillips, G. J., Hewitt, C. N., MacKenzie, A. R., Owen, S. M., Fowler, D., Heal, M. R., and Cape, J. N.: Direct ecosystem fluxes of volatile organic compounds from oil palms in South-East Asia, Atmos. Chem. Phys., 11, 8995–9017, doi:10.5194/acp-11-8995-2011, 2011.

Mogensen, D., Gierens, R., Crowley, J. N., Keronen, P., Smolander, S., Sogachev, A., Nölscher, A. C., Zhou, L., Kulmala, M., Tang, M. J., Williams, J., and Boy, M.: Simulations of atmospheric OH, O_3 and NO_3 reactivities within and above the boreal forest, Atmos. Chem. Phys., 15, 3909–3932, doi:10.5194/acp-15-3909-2015, 2015.

Monks, P. S., Granier, C., Fuzzi, S., Stohl, A.,Williams, M. L., Akimoto, H., Amann, M., Baklanov, A., Baltensperger, U., Bey, I., Blake, N., Blake, R. S., Carslaw, K., Cooper, O. R., Dentener, F., Fowler, D., Fragkou, E., Frost, G. J., Generoso, S., Ginoux, P., Grewe, V., Guenther, A., Hansson, H. C., Henne, S., Hjorth, J., Hofzumahaus, A., Huntrieser, H., Isaksen, I. S. A., Jenkin, M. E., Kaiser, J., Kanakidou, M., Klimont, Z., Kulmala, M., Laj, P., Lawrence, M. G., Lee, J. D., Liousse, C., Maione, M., McFiggans, G., Metzger, A., Mieville, A., Moussiopoulos, N., Orlando, J. J., O'Dowd, C. D., Palmer, P. I., Parrish, D. D., Petzold, A., Platt, U., Pöschl, U., Prévôt, A. S. H., Reeves, C. E., Reimann, S., Rudich, Y., Sellegri, K., Steinbrecher, R., Simpson, D., ten Brink, H., Theloke, J., van der Werf, G. R., Vautard, R., Vestreng, V., Vlachokostas, C., and von Glasow, R.: Atmospheric composition change – global and regional air quality, Atmos. Environ., 43, 5268–5350, doi:10.1016/j.atmosenv.2009.08.021, 2009.

Moore, C. J.: Frequency response corrections for eddy correlation systems, Bound.-Lay. Meteorol., 37, 17–35, 1986.

Müller, M., Graus, M., Ruuskanen, T. M., Schnitzhofer, R., Bamberger, I., Kaser, L., Titzmann, T., Hörtnagl, L., Wohlfahrt, G., Karl, T., and Hansel, A.: First eddy covariance flux measurements by PTR-TOF, Atmos. Meas. Tech., 3, 387–395, doi:10.5194/amt-3-387-2010, 2010.

Müller, M., Mikoviny, T., Jud, W., D'Anna, B., and Wisthaler, A.: A new software tool for the analysis of high resolution PTR-TOF mass spectra, Chemometr. Intell. Lab., 127, 158–165, 2013.

Nemitz, E., Hargreaves, K. J., Neftel, A., Loubet, B., Cellier, P., Dorsey, J. R., Flynn, M., Hensen, A., Weidinger, T., Meszaros, R., Horvath, L., Dämmgen, U., Frühauf, C., Löpmeier, F. J., Gallagher, M. W., and Sutton, M. A.: Intercomparison and assessment of turbulent and physiological exchange parameters of grassland, Biogeosciences, 6, 1445–1466, doi:10.5194/bg-6-1445-2009, 2009.

Owen, P. R. and Thompson, W. R.: Heat transfer across rough surfaces, J. Fluid Mech., 15, 321–334, 1963.

Paasonen, P., Asmi, A., Petäjä, T., Kajos, M. K., Äijälä, M., Junninen, H., Holst, T., Abbatt, J. P. D., Arneth, A., Birmili, W., van der Gon, H. D., Hamed, A., Hoffer, A., Laakso, L., Laaksonen, A., Leaitch, W. R., Plass-Dülmer, C., Pryor, S. C., Räisänen, P., Swietlicki, E., Wiedensohler, A., Worsnop, D. R., Kerminen, V.-M., and Kulmala, M.: Warming induced increase in aerosol number concentration likely to moderate climate change, Nat. Geosci., 6, 438–442, 2013.

Park, J.-H., Goldstein, A. H., Timkovsky, J., Fares, S., Weber, R., Karlik, J., and Holzinger, R.: Active atmosphere–ecosystem exchange of the vast majority of detected volatile organic compounds, Science, 9, 643–647, doi:10.1126/science.1235053, 2013.

Paulot, F., Wunch, D., Crounse, J. D., Toon, G. C., Millet, D. B., DeCarlo, P. F., Vigouroux, C., Deutscher, N. M., González Abad, G., Notholt, J., Warneke, T., Hannigan, J. W., Warneke, C., de Gouw, J. A., Dunlea, E. J., De Mazière, M., Griffith, D. W. T., Bernath, P., Jimenez, J. L., and Wennberg, P. O.: Importance of secondary sources in the atmospheric budgets of formic and acetic acids, Atmos. Chem. Phys., 11, 1989–2013, doi:10.5194/acp-11-1989-2011, 2011.

Peräkylä, O., Vogt, M., Tikkanen, O.-P., Laurila, T., Kajos, M. K., Rantala, P. A., Patokoski, J., Aalto, J., Yli-Juuti, T., Ehn, M., Sipilä, M., Paasonen, P., Rissanen, M., Nieminen, T., Taipale, R., Keronen, P., Lappalainen, H. K., Ruuskanen, T. M., Rinne, J., Kerminen, V.-M., Kulmala, M., Bäck, J., and Petäjä, T.: Monoterpenes' oxidation capacity and rate over a boreal forest: temporal variation and connection to growth of newly formed particles, Boreal Environ. Res., 19, 293–310, 2014.

Petäjä, T., Mauldin, III, R. L., Kosciuch, E., McGrath, J., Nieminen, T., Paasonen, P., Boy, M., Adamov, A., Kotiaho, T., and Kulmala, M.: Sulfuric acid and OH concentrations in a boreal forest site, Atmos. Chem. Phys., 9, 7435–7448, doi:10.5194/acp-9-7435-2009, 2009.

Potosnak, M. J., LeStourgeon, L., Pallardy, S. G., Hosman, K. P., Gu, L., Karl, T., Geron, C., and Guenther, A. B.: Observed and modeled ecosystem isoprene fluxes from an oak-dominated temperate forest and the influence of drought stress, Atmos. Environ., 84, 314–322, 2014.

Rantala, P., Taipale, R., Aalto, J., Kajos, M. K., Patokoski, J., Ruuskanen, T. M., and Rinne, J.: Continuous flux measurements of VOCs using PTR-MS – reliability and feasibility of disjunct-eddy-covariance, surface-layer-gradient, and surface-layer-profile methods, Boreal Environ. Res., 9, 87–107, 2014.

Rasmussen, R. A.: Isoprene: identified as a forest-type emission to the atmosphere, Environ. Sci. Technol., 4, 667–671, 1970.

Riemer, D., Pos, W., Milne, P., Farmer, C., Zika, R., Apel, E., Olszyna, K., Kliendienst, T., Lonneman, W., Bertman, S., Shepson, P., and Starn, T.: Observations of nonmethane hydrocarbons and oxygenated volatile organic compounds at a rural site in the southeastern United States, J. Geophys. Res.-Atmos., 103, 28111–28128, 1998.

Riipinen, I., Yli-Juuti, T., Pierce, J. R., Petäjä, T., Worsnop, D. R., Kulmala, M., and Donahue, N. M.: The contribution of organics to atmospheric nanoparticle growth, Nat. Geosci., 5, 453–458, 2012.

Rinne, J. and Ammann, C.: Disjunct eddy covariance method, in: Eddy Covariance Handbook, edited by: Aubinet, M., Vesala, T., and Papale, D., Springer, New York, USA, ISBN 978-94-007-2350-4, e-ISBN 978-94-007-2351-1, doi:10.1007/978-94-007-2351-1, 291–307, 2012.

Rinne, J., Guenther, A. B., Warneke, C., de Gouw, J. A., Luxembourg, S. L.: Disjunct eddy covariance technique for trace gas flux measurements, Geophys. Res. Lett., 28, 3139–3142, 2001.

Rinne, J., Taipale, R., Markkanen, T., Ruuskanen, T. M., Hellén, H., Kajos, M. K., Vesala, T., and Kulmala, M.: Hydrocarbon fluxes above a Scots pine forest canopy: measurements and modeling, Atmos. Chem. Phys., 7, 3361–3372, doi:10.5194/acp-7-3361-2007, 2007.

Rinne, J., Markkanen, T., Ruuskanen, T. M., Petäjä, T., Keronen, P., Tang, M.J., Crowley, J. N., Rannik, Ü., and Vesala, T.: Effect of chemical degradation on fluxes of reactive compounds – a study with a stochastic Lagrangian transport model, Atmos. Chem. Phys., 12, 4843–4854, doi:10.5194/acp-12-4843-2012, 2012.

Rivera-Rios, J. C., Nguyen, T. B., Crounse, J. D., Jud, W. St. Clair, J. M., Mikoviny, T., Gilman, J. B., Lerner, B. M., Kaiser, J. B., de Gouw, J., Wisthaler, A., Hansel, A., Wennberg, P. O., Seinfeld, J. H., and Keutsch, F. N.: Conversion of hydroperoxides to carbonyls in field and laboratory instrumentation: observational bias in diagnosing pristine versus anthropogenically controlled atmospheric chemistry, Geophys. Res. Lett., 41, 8645–8651, doi:10.1002/2014GL061919, 2014.

Roberts, J. M.: The atmospheric chemistry of organic nitrates, Atmos. Environ., 24A, 243–287, 1990.

Rosenstiel, T. N., Fisher, A. J., Fall, R., and Monson, R. K.: Differential accumulation of dimethylallyl diphosphate in leaves and needles of isoprene-and methylbutenol-emitting and nonemitting species, Plant Physiol., 129, 1276–1284, 2002.

Ruuskanen, T. M., Müller, M., Schnitzhofer, R., Karl, T., Graus, M., Bamberger, I., Hörtnagl, L., Brilli, F., Wohlfahrt, G., and Hansel, A.: Eddy covariance VOC emission and deposition fluxes above grassland using PTR-TOF, Atmos. Chem. Phys., 11, 611–625, doi:10.5194/acp-11-611-2011, 2011.

Saunders, S. M., Jenkin, M. E., Derwent, R. G., and Pilling, M. J.: Protocol for the development of the Master Chemical Mechanism, MCM v3 (Part A): tropospheric degradation of non-aromatic volatile organic compounds, Atmos. Chem. Phys., 3, 161–180, doi:10.5194/acp-3-161-2003, 2003.

Singh, H. B., O'Hara, D., Herlth, D., Sachse, W., Blake, D. R., Bradshaw, J. D., Kanakidou, M., and Crutzen, P. J.: Acetone in the atmosphere: distribution, sources, and sinks, J. Geophys. Res., 99, 1805–1819, doi:10.1029/93JD00764, 1994.

Singh, H. B., Kanakidou, M., Crutzen, P. J., and Jacob, D. J.: High concentrations and photochemical fate of oxygenated hydrocarbons in the global troposphere, Nature, 378, 50–54, 1995.

Taipale, R., Ruuskanen, T. M., and Rinne, J.: Lag time determination in DEC measurements with PTR-MS, Atmos. Meas. Tech., 3, 853–862, doi:10.5194/amt-3-853-2010, 2010.

Tunved, P., Hansson, H.-C., Kerminen, V.-M., Ström, J., Dal Maso, M., Lihavainen, H., Viisanen, Y., Aalto, P. P., Komppula, M., and Kulmala, M.: High natural aerosol loading over boreal forests, Science, 312, 261–263, 2006.

Warneke, C., Luxembourg, S. L., de Gouw, J. A., Rinne, J., Guenther, A. B., and Fall, R.: Disjunct eddy covariance measurements of oxygenated volatile organic compounds fluxes from an alfalfa field before and after cutting, J. Geophys. Res., 107, ACH-6-1–ACH-6-10, doi:10.1029/2001JD000594, 2002.

Willmott, C. J. and Matsuura, K.: Terrestrial Air Temperature: 1900–2010 Gridded Monthly Time Series, Version 3.01, available at: http://climate.geog.udel.edu/~climate/html_pages/Global2011/README.GlobalTsT2011.html (last access: 21 August 2015), 2012a.

Willmott, C. J. and Matsuura, K.: Terrestrial Precipitation: 1900–2010 Gridded Monthly Time Series, Version 3.01, available at: http://climate.geog.udel.edu/~climate/html_pages/Global2011/README.GlobalTsP2011.html (last access: 21 August 2015), 2012b.

Wohlfahrt, G., Amelynck, C., Ammann, C., Arneth, A., Bamberger, I., Goldstein, A. H., Gu, L., Guenther, A., Hansel, A., Heinesch, B., Holst, T., Hörtnagl, L., Karl, T., Laffineur, Q., Neftel, A., McKinney, K., Munger, J. W., Pallardy, S. G., Schade, G. W., Seco, R., and Schoon, N.: An ecosystem-scale perspective of the net land methanol flux: synthesis of micrometeorological flux measurements, Atmos. Chem. Phys. Discuss., 15, 2577–2613, doi:10.5194/acpd-15-2577-2015, 2015.

Table 1. Comparison between the classical and the automated method for calculating VOC fluxes.

Step	Classical	Automated
Standard flux corrections	yes	yes
Calculate cross covariance function (CCF)	yes	yes
Manual evaluation of CCFs (several 100)	yes	no
Average absolute CCFs	no	yes
Data used for CCF plot and flux detection	30 min	$86 \cdot 30$ min
Threshold dependent results (σ_{noise})	no	yes
Filter results (fragments, isotopes, clusters)	yes	no
Work intensive	yes	no
Maximum of found flux-masses in literature	10–20	ca. 500

Table 2. Depositions (*D*) and emissions (*E*) calculated with different methods.

possible compound	mass (prot.) Th	elemental composition	classical method		automated method		automated method with compound filter	
			% of total emission (*E*) or deposition (*D*)					
			D (−0.28)[a]	*E* (8.5)[a]	*D* (−0.47)[a]	*E* (10.5)[a]	*D* (−0.44)[a]	*E* (9.5)[a]
isoprene[c]	69.0699	$C_5H_9^+$	0.2	75.0	0.0	61.2	0.0	67.7
methanol[c]	33.0335	$C_1H_5O_1^+$	97.2	18.4	77.1	14.5	83.1	16.1
acetone[c]	59.0491	$C_3H_7O_1^+$			2.1	3.3	2.3	3.6
MVK/MACR[c]	71.0491	$C_4H_7O_1^+$	1.1	3.9	1.0	3.0	1.1	3.3
monoterpenes[c]	137.1325	$C_{10}H_{17}^+$	0.2	2.6	0.1	2.1	0.1	2.3
acetaldehyde[c]	45.0335	$C_2H_5O_1^+$			0.1	2.2	0.1	2.4
acetic acid	61.0284	$C_2H_5O_2^+$			10.5	1.5	11.3	1.6
acrolein[c]	57.0335	$C_3H_5O_1^+$			0.4	0.8	0.4	0.9
methyl acetate	75.0441	$C_3H_7O_2^+$			1.0	0.7	1.1	0.8
butanone[c]	73.0648	$C_4H_9O_1^+$			0.3	0.7	0.3	0.8
C_6 GLV *F*[d]	83.0855	$C_6H_{11}^+$			0.0	0.3	0.0	0.4
pentanal	85.0648	$C_5H_9O_1^+$			0.2	0.2	0.2	0.2
unknown	101.0597	$C_5H_9O_2^+$	1.2	0.1				
CH *F*[b]	41.0386	$C_3H_5^+$			0.3	4.8		
monot *F*[b]	81.0699	$C_6H_9^+$			0.1	1.1		
CHO *F*[b]	43.0178	$C_2H_3O_1^+$			6.1	1.5		
methanol WC[b]	51.0441	$C_1H_7O_2^+$			0.4	1.0		
isop. *F*[b]	67.0542	$C_5H_7^+$			0.2	0.6		
isop. CT[b]	68.0621	$C_5H_8^+$			0.1	0.5		
monot. *F*[b]	95.0855	$C_7H_{11}^+$			0.1	0.1		

[a] Total *E* or *D* in $\mathrm{nmol\,m^{-2}\,s^{-1}}$;
[b] *F*: fragment, WC: watercluster, CT: charge transfer;
[c] calibrated compounds;
[d] C_6 green leaf volatiles (GLV) are calculated via the fragment $C_6H_{11}^+$. The fragmentation pattern and the sensitivity of hexanal were used.

Table 3. Deposited compounds, their daily averaged concentration, the maximum diurnal deposition and their respective lifetimes.

compound	concentration [ppb]	deposition [nmol m^{-2} s^{-1}]	lifetime [days]
methanol	14.3	−2.7	7[a]
acetic acid	2.5	−0.4	1.7[b]
acetone	4.7	−0.1	15[c]

[a] Atmospheric lifetime according do Jacob et al. (2005).
[b] Lifetime in the boundary layer according to Paulot et al. (2011).
[c] Tropospheric lifetime according to Jacob et al. (2002).

Title Page
Abstract Introduction
Conclusions References
Tables Figures
◀◀ ▶▶
◀ ▶
Back Close
Full Screen / Esc
Printer-friendly Version
Interactive Discussion

Figure 1. Satellite picture (Imagery©2015 Cnes/Spot Image, DigitalGlobe, European Space Imaging, Landsat, Map data ©2015 Google) of the Bosco Fontana national park and the surroundings. The position of the flux tower is marked by a white cross. The dark green surrounding is the forest area of the national park.

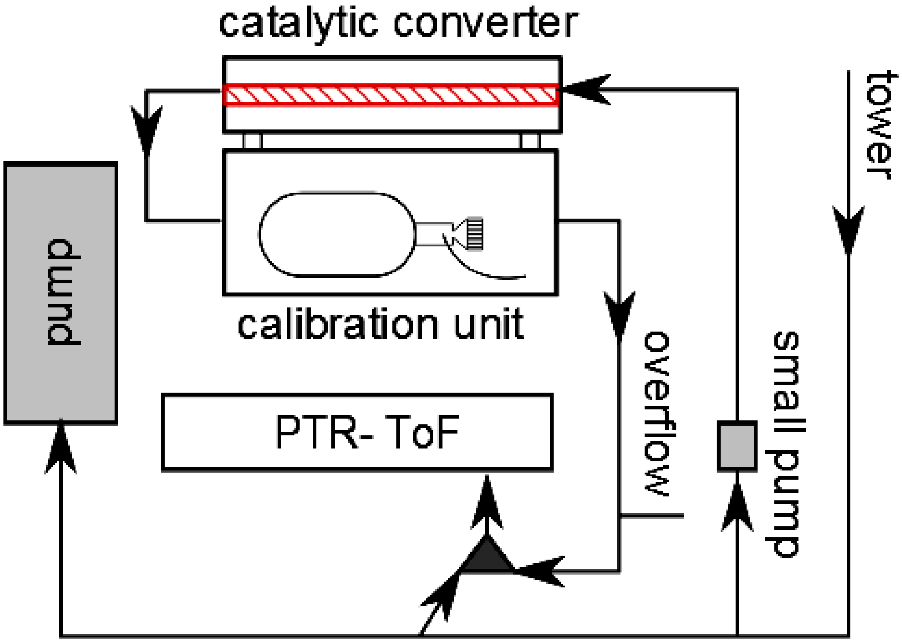

Figure 2. Schematic sketch of the inlet of the PTR-TOF used for the VOC measurements.

ACPD
15, 27627–27673, 2015

Characterization of total ecosystem scale biogenic VOC exchange

S. Schallhart et al.

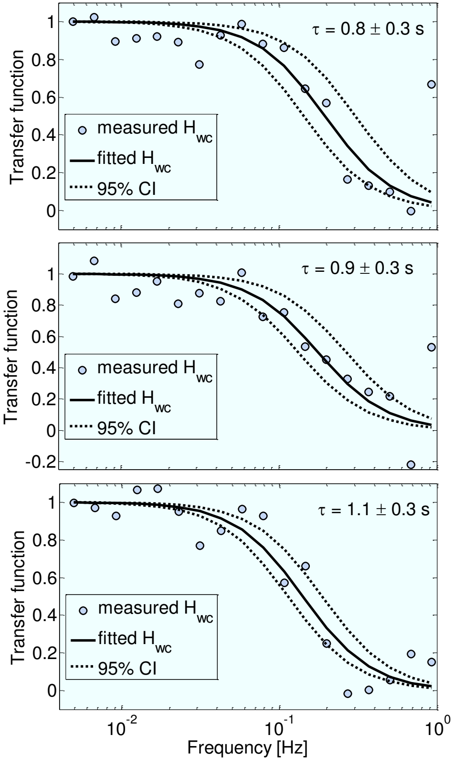

Figure 3. Transfer functions of $H_3O^+H_2O$ (37.0284 amu; top), H_3O^+ $(H_2O)_2$ (55.039 amu; middle) and $C_5H_8H^+$ (69.0699 amu; bottom). The circles are the measurents, the solid black line the fitted transfer function and the dashed lines are the 95 % confidence intervals. The response time of the measurement system, τ, was calculated by fitting Eq. (10) to the data.

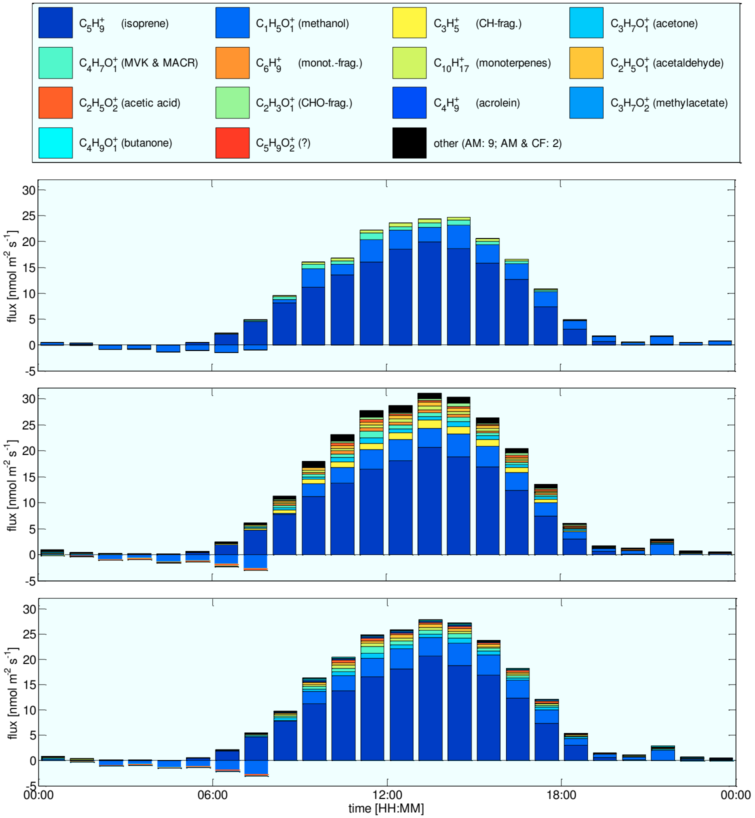

Figure 4. Diurnal flux plot of the classical method (top panel), the automated method (mid) and the automated method with compound filter (bottom panel). The time is in UTC + 1 h. In each panel the 10 most abundend flux compounds are shown, the remaining compounds are summed up and plotted as “other”. For the automated method (AM) there were 9 compounds summed up, for the automated method with compound filter (AM & CF) there were 2. All flux compounds are listed in Table 2.

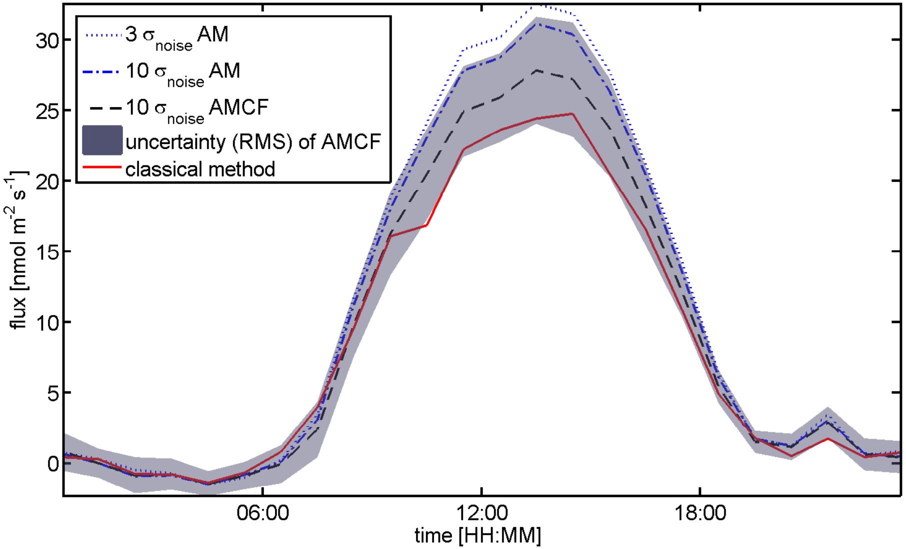

Figure 5. Diurnal average of the automated method (AM) with 3 and $10\sigma_{\text{noise}}$ threshold for the flux calculation, the automated method with compound filter (AMCF) using a $10\sigma_{\text{noise}}$ threshold, its uncertainty (root mean square) and the classical method. The time is in UTC + 1 h.

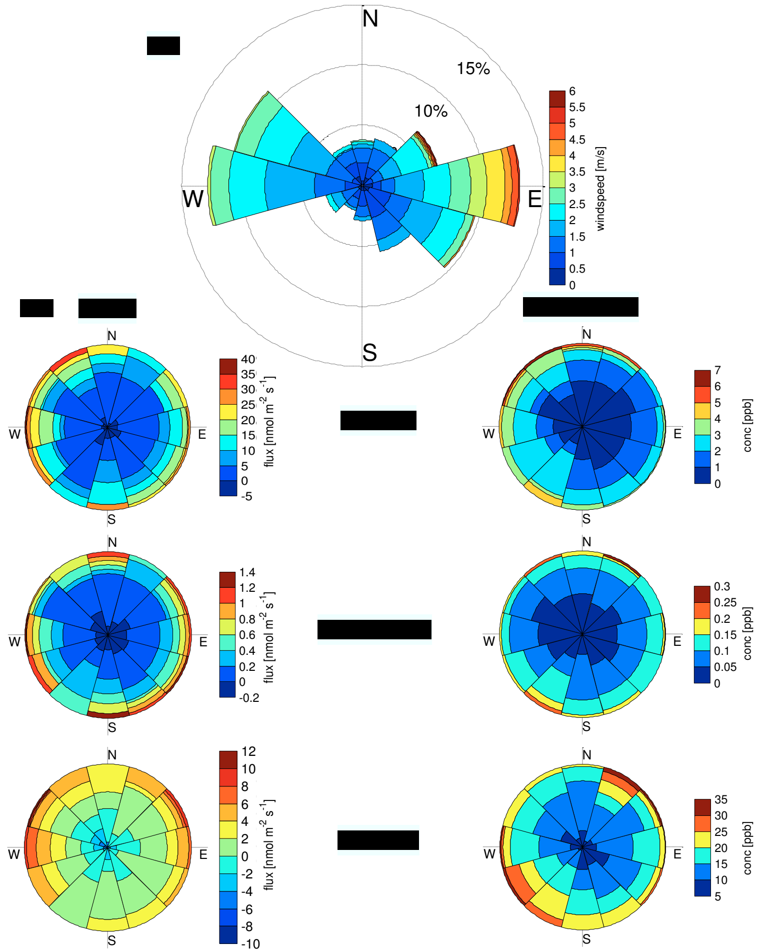

Figure 6. (a) Wind rose of the wind speed. **(b)** Unscaled wind roses for fluxes (left) and concentrations (right) of isoprene (top), monoterpenes (mid), methanol (bottom).

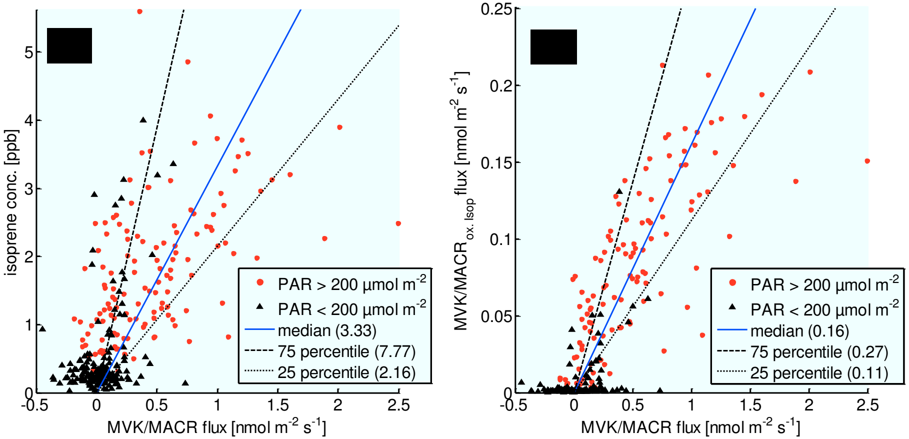

Figure 7. Scatter plots of the isoprene concentration and the MVK/MACR flux **(a)** and the calculated MVK/MACR flux from oxidation of isoprene and the MVK/MACR flux **(b)**. The 1 h data are separated to day and night values by a 200 µmol m^{-2} photo active radiation (PAR) threshold. The $\frac{y}{x}$ ratios of the daytime data have been calculated for the two figures, respectively. From those ratios the median, 25 and 75 % iles have been calculated. The correlation factors for the day and night data are 0.65 in plot **(a)** and 0.81 in plot **(b)**. The MVK/MACR flux from oxidation of isoprene was calculated using Eq. (14).

Title Page
Abstract | Introduction
Conclusions | References
Tables | Figures
◂◂ | ▸▸
◂ | ▸
Back | Close
Full Screen / Esc
Printer-friendly Version
Interactive Discussion

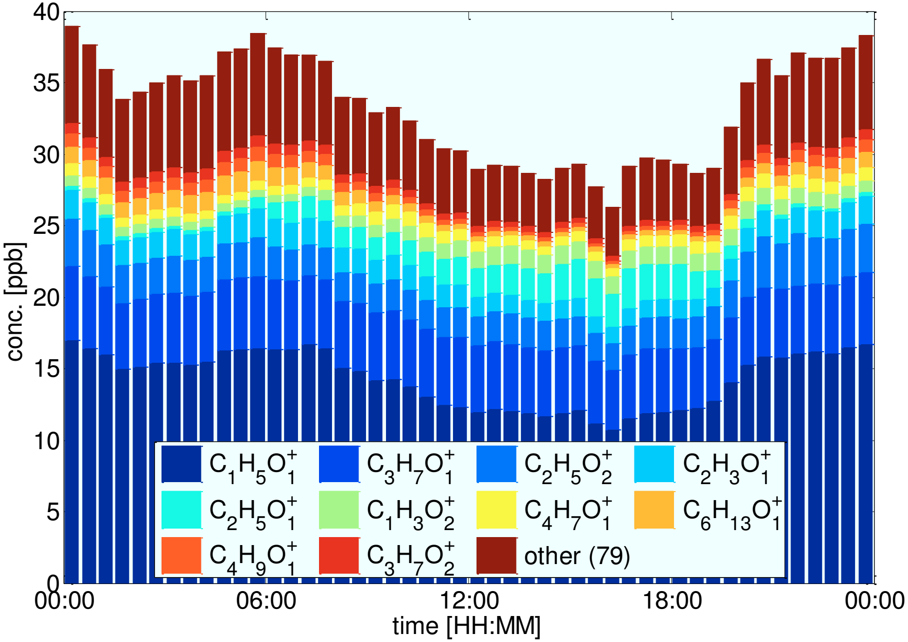

Figure 8. Diurnal average of the total VOC concentration resolved with the PTR-ToF (filtered for fragments). The 10 most abundend flux compounds are shown, the remaining compounds are summed up and plotted as "other".The time is in CET wintertime.

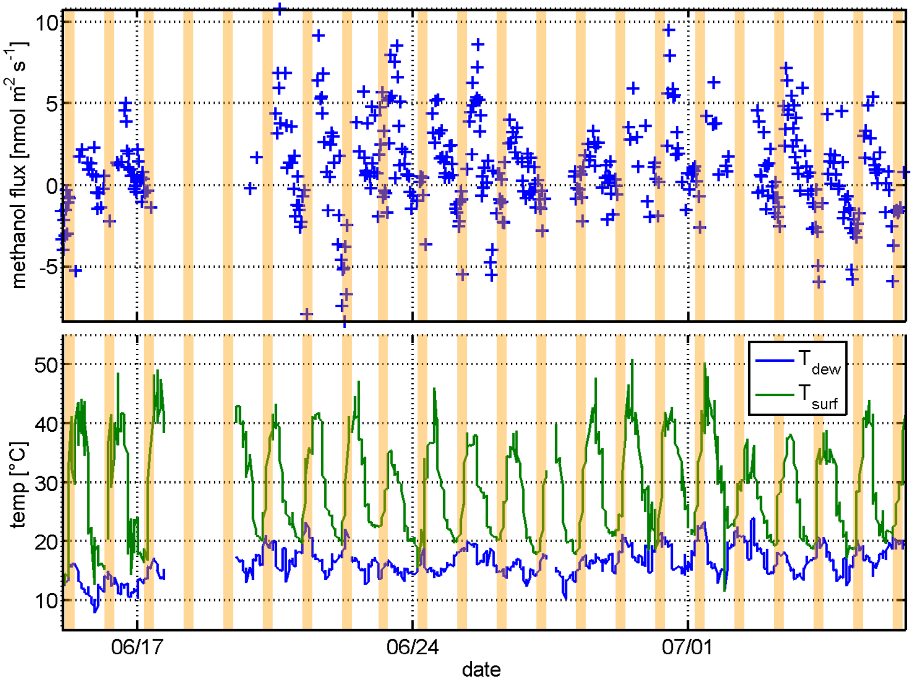

Figure 9. Time series of the methanol flux (top panel) and the calculated surface (T_{surf}) and dew point temperature (T_{dew}; bottom panel). The periods between 01:00 and 08:00 CET wintertime (methanol deposition from the diurnal plot, Fig. 4) are highlighted with yellow.